

Are your **MRI contrast agents** cost-effective?

Learn more about generic **Gadolinium-Based Contrast Agents**.



**FRESENIUS
KABI**

caring for life

AJNR

Mapping Human Fetal Brain Maturation in Vivo Using Quantitative MRI

V.U. Schmidbauer, G.O. Dovjak, M.S. Yildirim, G. Mayr-Geisl, M. Weber, M.C. Diogo, G.M. Gruber, F. Prayer, R.-I. Milos, M. Stuempflen, B. Ulm, J. Binder, D. Bettelheim, H. Kiss, D. Prayer and G. Kasprian

This information is current as of April 18, 2024.

AJNR Am J Neuroradiol published online 9 September 2021
<http://www.ajnr.org/content/early/2021/09/09/ajnr.A7286>

Mapping Human Fetal Brain Maturation in Vivo Using Quantitative MRI

V.U. Schmidbauer, G.O. Dovjak, M.S. Yildirim, G. Mayr-Geisl, M. Weber, M.C. Diogo, G.M. Gruber, F. Prayer, R.-I. Milos, M. Stuempflen, B. Ulm, J. Binder, D. Bettelheim, H. Kiss, D. Prayer, and G. Kasprian



ABSTRACT

BACKGROUND AND PURPOSE: On the basis of a single multidynamic multiecho sequence acquisition, SyMRI generates a variety of quantitative image data that can characterize tissue-specific properties. The aim of this retrospective study was to evaluate the feasibility of SyMRI for the qualitative and quantitative assessment of fetal brain maturation.

MATERIALS AND METHODS: In 52 fetuses, multidynamic multiecho sequence acquisitions were available. SyMRI was used to perform multidynamic multiecho-based postprocessing. Fetal brain maturity was scored qualitatively on the basis of SyMRI-generated MR imaging data. The results were compared with conventionally acquired T1-weighted/T2-weighted contrasts as a standard of reference. Myelin-related changes in T1-/T2-relaxation time/relaxation rate, proton density, and MR imaging signal intensity of the developing fetal brain stem were measured. A Pearson correlation analysis was used to detect correlations between the following: 1) the gestational age at MR imaging and the fetal brain maturity score, and 2) the gestational age at MR imaging and the quantitative measurements.

RESULTS: SyMRI provided images of sufficient quality in 12/52 (23.08%) (range, 23 + 6–34 + 0) fetal multidynamic multiecho sequence acquisitions. The fetal brain maturity score positively correlated with gestational age at MR imaging (SyMRI: $r = 0.915$, $P < .001$ /standard of reference: $r = 0.966$, $P < .001$). Myelination-related changes in the T2 relaxation time/T2 relaxation rate of the medulla oblongata significantly correlated with gestational age at MR imaging (T2-relaxation time: $r = -0.739$, $P = .006$ /T2-relaxation rate: $r = 0.790$, $P = .002$).

CONCLUSIONS: Fetal motion limits the applicability of multidynamic multiecho-based postprocessing. However, SyMRI-generated image data of sufficient quality enable the qualitative assessment of maturity-related changes of the fetal brain. In addition, quantitative T2 relaxation time/T2 relaxation rate mapping characterizes myelin-related changes of the brain stem prenatally. This approach, if successful, opens novel possibilities for the evaluation of structural and biochemical aspects of fetal brain maturation.

ABBREVIATIONS: GA = gestational age; MDME = multidynamic multiecho; PD = proton density; R1 = T1-relaxation rate; R2 = T2-relaxation rate; SI = signal intensity; T1R = T1-relaxation time; T2R = T2-relaxation time

Ultrasonography is considered the mainstay of antenatal imaging and serves as the technique of choice for the structural examination of the human fetus in utero.¹⁻⁵ However, the sonography-based assessment of prenatal brain development has some specific limitations.⁶⁻⁹ Foremost among these is that current

sonography imaging systems do not allow a tissue-specific quantitative characterization of fetal brain maturity.¹⁰

Physical MR imaging properties have been proved to provide noninvasive biomarkers for the assessment of brain maturation¹¹ and may offer new possibilities in the prenatal detection of neurodevelopmental anomalies. Until now, the acquisition of quantitative parameters, underlying visually perceptible MR imaging signal intensity (SI) values, was considered a highly time-consuming process, which limited its applicability in a clinical setting.¹²⁻¹⁶ Recent developments in quantitative MR imaging enable the generation of various MR imaging contrasts and quantitative maps based on a single multidynamic multiecho (MDME) sequence acquisition and, therefore, in a clinically acceptable imaging time.¹⁷⁻¹⁹ The MDME data-postprocessing software SyMRI (Synthetic MR AB; Version 11.1.5) provides information about tissue-specific MR imaging properties such as proton density (PD) and relaxation

Received April 17, 2021; accepted after revision July 19.

From the Departments of Biomedical Imaging and Image-Guided Therapy (V.U.S., G.O.D., M.S.Y., M.W., M.C.D., F.P., R.-I.M., M.S., D.P. G.K), Neurosurgery (G.M.-G.), and Obstetrics and Gynecology (B.U., J.B., D.B., H.K.), Medical University of Vienna, Vienna, Austria; and Department of Anatomy and Biomechanics (G.M.G.), Karl Landsteiner University of Health Sciences, Krems an der Donau, Austria.

Paper previously presented at: Annual Meeting of the European Congress of Radiology, March 3–7, 2021; Virtual.

Please address correspondence to Gregor Kasprian, MD, Department of Biomedical Imaging and Image-Guided Therapy, Medical University of Vienna, Waehringer Guertel 18-20, 1090 Vienna, Austria; e-mail: gregor.kasprian@meduniwien.ac.at

Indicates article with online supplemental data.

<http://dx.doi.org/10.3174/ajnr.A7286>

Demographics and clinical characteristics

Fetal MDME Sequence Acquisitions (n = 12)	GA at MR Imaging	Sex	Position	Brain MR Imaging Findings
1	23 + 6	♀	Breech	Dolichocephaly
2	24 + 6	♂	Cephalic	Asymmetry of lateral ventricles
3	25 + 4	♂	Cephalic	No pathologic findings
4	25 + 4	♂	Cephalic	No pathologic findings
5	25 + 5	♀	Cephalic	No pathologic findings
6	25 + 5	♂	Breech	Altered signal of periventricular crossroads
7	26 + 6	♀	Cephalic	No pathologic findings
8	27 + 4	♂	Breech	No pathologic findings
9	29 + 6	♂	Cephalic	No pathologic findings
10	30 + 1	♂	Breech	No pathologic findings
11	32 + 4	♀	Cephalic	Agnesis of septum pellucidum
12	34 + 0	♀	Cephalic	Agnesis of corpus callosum, ventriculomegaly, hemorrhage (left cella media)

parameters (T1-relaxation time [T1R]/T1-relaxation rate [R1]; T2-relaxation time [T2R]/T2-relaxation rate [R2]).¹⁷ Furthermore, this method allows the adjustment of TR, TE, and TI in retrospect, which enables an individual modulation of the MR imaging contrasts after data acquisition.¹⁹ MDME-based imaging proved beneficial in a neonatal neuroimaging setting because this technique allows a reduction in examination time, while providing a variety of imaging data beyond the standard neonatal MR imaging protocol.^{11,15,16} However, currently, the full potential of this technology for the investigation of brain maturation at early developmental stages is widely unexplored.

The aim of this study was to evaluate the feasibility of quantitative MDME-based postprocessing for human fetal brain imaging. For this purpose, qualitative neuroradiologic assessments of brain maturation based on SyMRI-generated and conventionally acquired MR imaging data were compared. The visual evaluation of fetal brain maturity was complemented by a self-assessment of confidence by the investigating radiologists. In addition, tissue-specific properties of the fetal brain stem were quantified, to investigate whether the described approach is sensitive to the detection of myelin-related changes.

MATERIALS AND METHODS

Ethics Approval

The Ethics Commission of the Medical University of Vienna approved the protocol of this study. All women provided written informed consent for fetal MR imaging before scanning and agreed to the scientific use of the acquired data.

Study Cohort

Between December 2019 and October 2020, a total of 52 fetal MR images, including MDME sequence acquisitions of the fetal brain, were collected at the Neuroradiology Department of a tertiary care

hospital. All fetuses included in this study were referred for MR imaging by the Department of Obstetrics and Gynecology after a detailed sonographic examination by a fetal medicine specialist, according to European standards. Congenital abnormalities of the central nervous system were the most common indications for fetal MR imaging (Online Supplemental Data). A detailed overview of demographic and clinical characteristics of included fetuses is given in the Table. Fetal gestational age (GA) (weeks) was determined at the first trimester ultrasonographic screening.

Fetal MR Imaging Data Acquisition and SyMRI-Based MDME Postprocessing

Imaging was performed in accordance with the fetal MR imaging guidelines of the International Society of Sonography in Obstetrics and Gynecology.²⁰ All fetuses were examined using a standardized fetal MR imaging protocol of the brain (Online Supplemental Data) on the same Ingenia 1.5T MR imaging system (Philips Healthcare) equipped with a body coil. An MDME sequence (Online Supplemental Data) (acquisition time: 3 minutes and 20 seconds) was acquired (axial plane) by applying 2 repeat acquisition phases: phase a: saturation of 1 section by a section-selective saturation pulse (flip angle = 120°); and phase b: section-selective excitation pulses (flip angle = 90°) and section-selective refocusing pulses (flip angle = 180°) to generate a train of spin-echoes for another section.^{17,21,22} Via the mismatch between the saturated section and the image section, a matrix with a variety of effects of R1/R2 was acquired.^{21,22} Echo-trains, characterized by different saturation delays, were used to estimate T1-/T2-relaxation parameters.^{17,21,22}

The T1-relaxation constants allowed the local radiofrequency field (B₁) to be calculated.²¹ On the basis of the acquired relaxation parameters and B₁, the PD can be computed.¹⁷ SyMRI-based MDME postprocessing (postprocessing time: <1 minute) was applied to generate conventional MR imaging contrasts (Fig 1) and quantitative MR imaging maps (Fig 2) for qualitative and quantitative analysis. Color-coded voxels, according to the physical MR imaging properties, were used to generate quantitative maps.²¹

Fetal Brain Maturity Assessment

Before the evaluation of the MR imaging data, a visual review was performed. On the basis of the subjective judgment made by 1 fetal imaging specialist with 15 years of experience, fetuses were excluded from this study if qualitative and quantitative analyses were not possible due to severely degraded images by fetal motion. To assess fetal brain maturity, we used a qualitative scoring system based on existing brain-maturation scores.^{15,23} Developmental aspects were evaluated on both conventionally acquired MR imaging contrasts (T1-weighted/snapshot inversion recovery, T2-weighted) (axial plane) and SyMRI-generated image

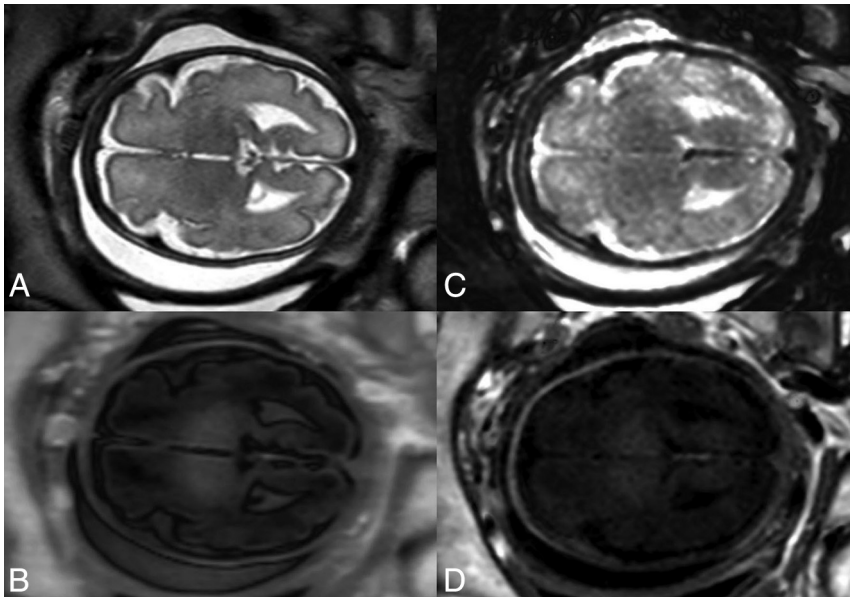


FIG 1. Conventionally acquired (A and B) and SyMRI-generated (C and D) fetal MR image data of comparable SIs: T2-weighted (A); snapshot inversion recovery (B); T2-weighted STIR (TR = 15000 ms, TE = 100 ms, TI = 300 ms) (C); and T1-weighted inversion recovery (TR = 2500 ms, TE = 10 ms, TI = 1050 ms) (D). Presentation of SyMRI-generated MR imaging contrasts based on the default software settings for TR, TE, and TI.

data (T1-weighted/T1-weighted inversion recovery, T2-weighted/T2-weighted STIR, quantitative MR imaging maps) (axial plane) by 2 independent neuroradiologists (rater 1, with 15 years of experience, and rater 2, with 30 years of experience with fetal MR imaging), who were blinded to GA at MR imaging. The criteria used to determine brain maturity were the following: morphologic presentation of the frontal, occipital, and insular cortices according to Vossough et al;²³ the presence of the germinal matrix; identifiability of the primary sulci;²⁴ and fetal brain myelination (medulla oblongata, midbrain and inferior colliculus, thalamus, posterior limb of the internal capsule, and central region).¹⁵

SyMRI-generated quantitative MR imaging maps based on T1R/R1 and T2R/R2 were available for the assessment of brain myelination. The observers had the opportunity to adjust the windowing (conventionally acquired and SyMRI-generated MR imaging contrasts); TR, TE, and TI (SyMRI-generated MR imaging contrasts); and the color-coding scale (SyMRI-generated quantitative MR imaging maps) at their discretion during fetal brain maturity assessment. The scoring system is explained in the Online Supplemental Data. The points allocated for each evaluated developmental aspect were totaled, resulting in a fetal brain maturity total score for each included subject. Furthermore, both raters performed a Likert scale-based self-assessment of confidence with regard to the evaluation of fetal brain maturity. For this purpose, both raters allocated a minimum of 1 (not very confident) and a maximum of 4 (highly confident) points when assessing the 10 components of the score. The allocated points were totaled, resulting in a total score for confidence (minimum: 10 [lowest level of confidence]; maximum: 40 [highest level of confidence]) for each included subject.

Determination of Physical Properties of the Brain Stem

T1R (ms), R1 (s^{-1}), T2R (ms), R2 (s^{-1}), PD (%), and MR imaging SI values were determined by manual delineation of the medulla oblongata and the midbrain on SyMRI-generated image data (T1R/R1, T2R/R2, PD) and conventionally acquired T2-weighted contrasts (MR imaging SI values) (axial plane). The provided average values of the physical properties were calculated on the basis of the voxels within the drawn ROI. The ROI placement (Online Supplemental Data) was performed separately from fetal brain maturity assessment by 2 different investigators (investigator 1, with 2 years of experience and investigator 2, with 1 year of experience with fetal MR imaging), who were blinded to GA at MR imaging.

Statistical Analyses

Statistical analyses were performed using SPSS Statistics for Macintosh,

Version 25.0 (2017; IBM) at a significance level of $\alpha = 5\%$ ($P < .05$).

To detect concordances of the fetal brain maturity assessment of both raters and the quantitative measurements of both investigators, we calculated an intraclass correlation coefficient. The intraclass correlation coefficient values of ≥ 0.75 were considered a strong correlation.²⁵ In case of high concordances, the results of 1 rater were reported.

Pearson correlation analyses were performed to assess correlations between the GA at MR imaging and the fetal brain maturity total score, and the quantitative measurements of the fetal brain stem.

RESULTS

Feasibility of SyMRI for Human Fetal Brain Imaging

Image data perceived to be of sufficient quality for qualitative and quantitative analysis were provided in 12/52 (23.08%) (mean GA at fetal MR imaging: 27 + 5 [SD, 3 + 1] weeks; range, 23 + 6–34 + 0 weeks) fetal MDME sequence acquisitions (Table and Online Supplemental Data). In 40/52 (76.92%) cases, the image quality of SyMRI-generated image data was highly degraded by fetal motion (Online Supplemental Data).

Interrater Reliability

There was a strong correlation between the fetal brain maturity total score assessed by both raters on SyMRI-generated MR imaging data, 0.798 (95% CI, 0.279–0.943). There was no strong correlation between the fetal brain maturity total score assessed by both raters on conventionally acquired MR imaging data, 0.587 (95% CI, –0.055–0.898). There were strong correlations between the quantitative measurements determined by both investigators,

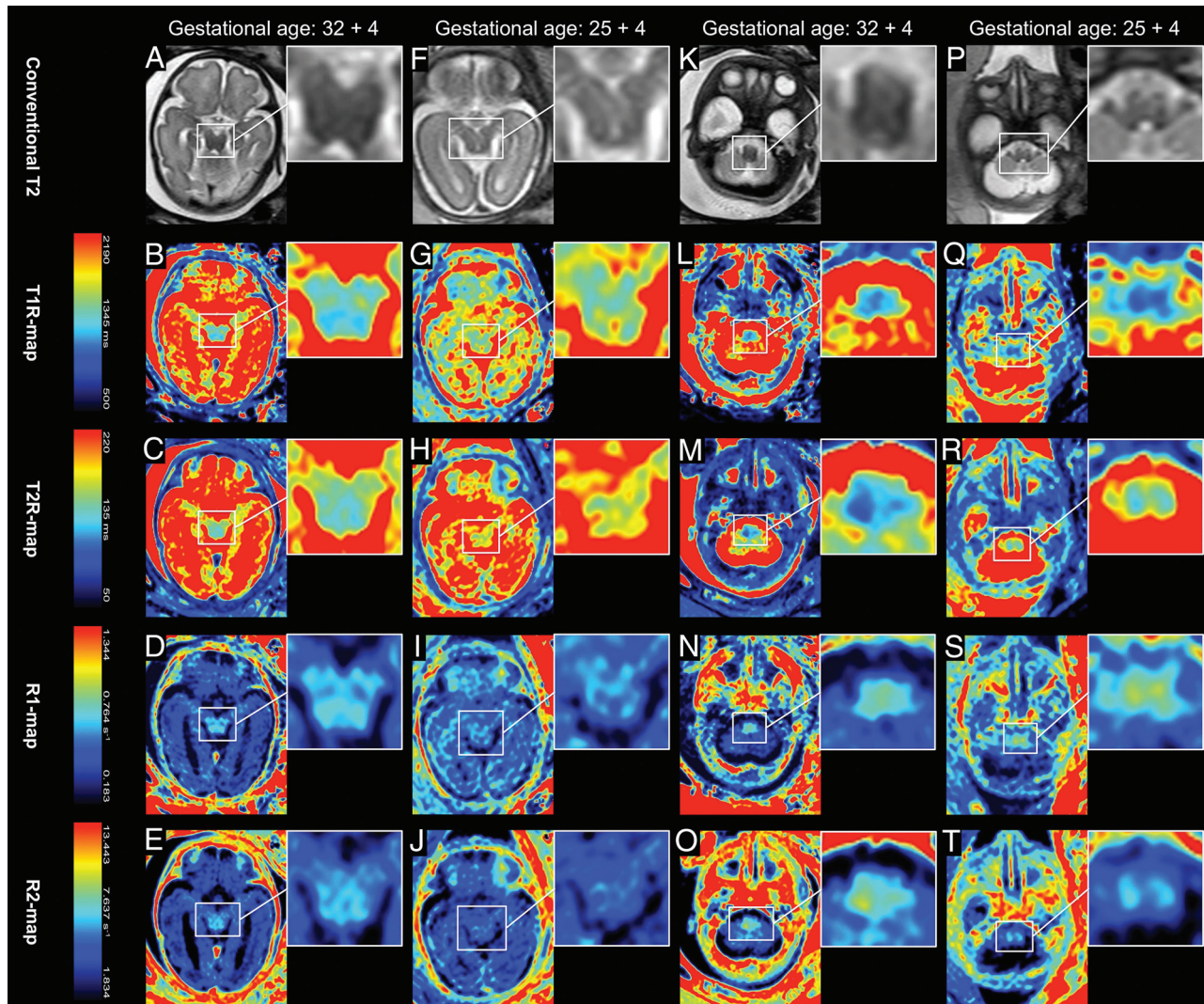


FIG 2. Presentation of conventionally acquired T2-weighted MR imaging contrasts (A, F, K, P) and quantitative MR imaging maps based on T1R (B, G, L, Q), T2R (C, H, M, R), R1 (D, I, N, S), and R2 (E, J, O, T). The color-coding, according to the T1-/T2-relaxation parameters, is indicated by the colored bars. The first (A, B, C, D, E) and the third columns (K, L, M, N, O) show MR imaging data from a fetus imaged at 32 + 4 weeks' GA. The second (F, G, H, I, J) and the fourth columns (P, Q, R, S, T) show MR imaging data from a fetus imaged at 25 + 4 weeks' GA. Brain myelination is indicated by a shortening of T1R/T2R (blue color-coding) and a prolongation of R1/R2 (yellow/orange color-coding). The color-coding of T1-relaxation parameters shows a distinct myelination of the medulla oblongata (L, N) and the midbrain tegmentum/tectum (B, D) at 32 + 4 weeks' GA. At 25 + 4 weeks' GA, only the medulla oblongata shows remarkable myelination (Q, S). The color-coding of T2-relaxation parameters indicates myelination of the medulla oblongata (M, O) at 32 + 4 weeks' GA. Beginning T2R-shortening and R2-prolongation are visible in the medulla oblongata (R, T) at 25 + 4 weeks' GA and in the midbrain tegmentum/tectum (C, E) at 32 + 4 weeks' GA.

ranging from 0.879 (95% CI, 0.643–0.963) to 0.989 (95% CI, 0.962–0.997) (Online Supplemental Data).

Assessment of Fetal Brain Maturity

The fetal brain maturity total score based on the assessment of SyMRI-generated MR imaging data showed a positive correlation with the GA at fetal MR imaging ($r = 0.915$, $P < .001$). The fetal brain maturity total score based on the assessment of conventionally acquired MR imaging data showed a positive correlation with the GA at fetal MR imaging (rater 1: $r = 0.966$, $P < .001$; rater 2: $r = 0.915$, $P < .001$) (Fig 3 and Online Supplemental Data).

The self-assessment of confidence by the investigating radiologists revealed a higher level of confidence for the assessment of fetal brain maturity on the basis of conventionally acquired MR

imaging data (rater 1: median, 34; range, 33–34; and rater 2: median, 34.5; range, 31–40) compared with SyMRI-generated MR imaging data (rater 1: median, 32.5; range, 19–38. and rater 2: median, 33; range, 16–34) (Online Supplemental Data).

Physical Tissue Properties of the Brain Stem

Significant correlations were observed between the GA at fetal MR imaging and the T2R ($r = -0.739$, $P = .006$) and R2 ($r = 0.790$, $P = .002$) determined in the medulla oblongata. No significant correlations were observed between the GA at fetal MR imaging and the T1R ($r = -0.340$, $P = .280$), R1 ($r = 0.467$, $P = .126$), PD ($r = -0.071$, $P = .826$), or MR imaging SI ($r = -0.264$, $P = .408$) determined in the medulla oblongata. No significant correlations were observed between the GA at fetal MR imaging and the T1R ($r =$

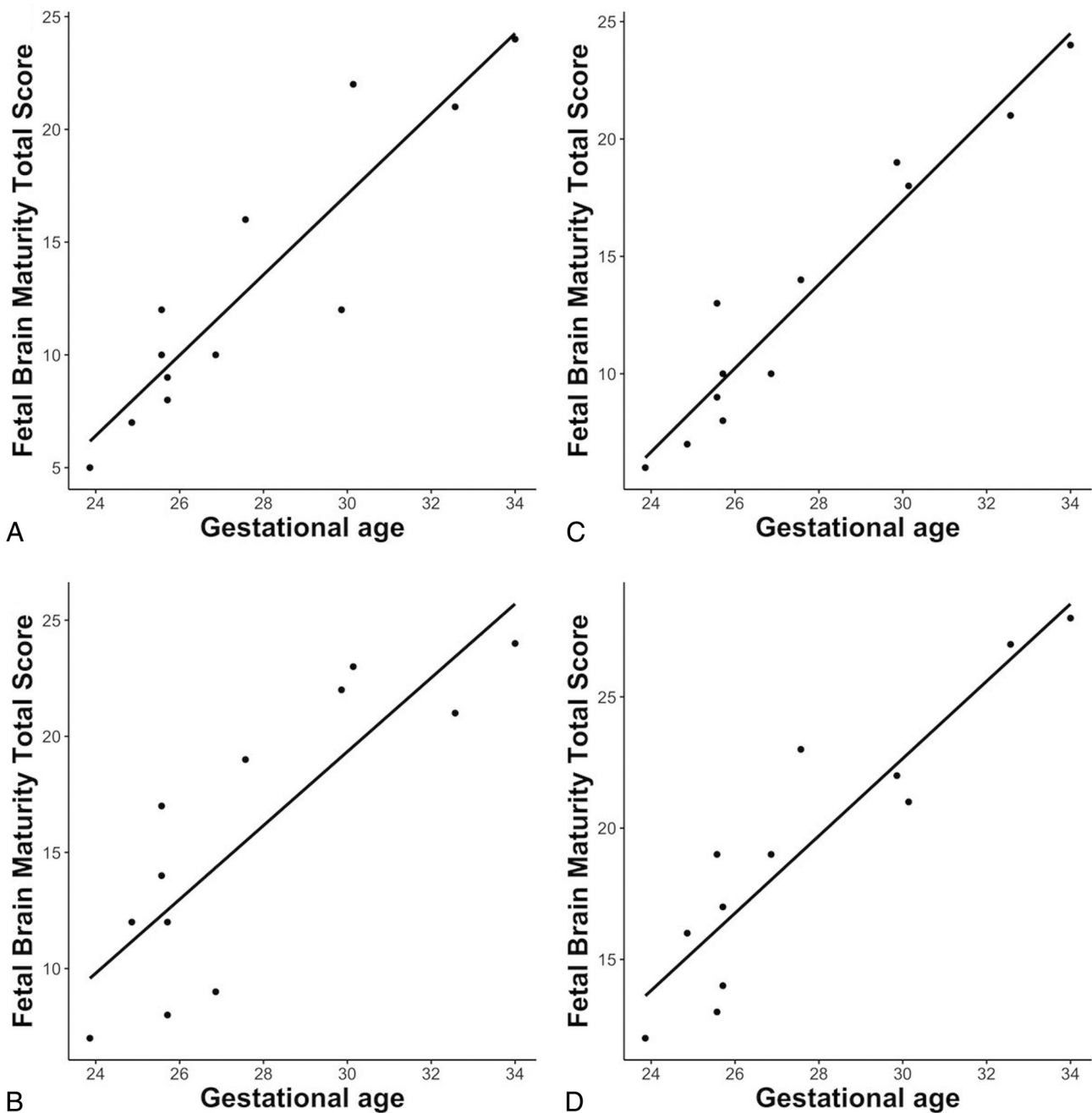


FIG 3. Pearson correlation between GA at MR imaging (x-axis) and the fetal brain maturity total score (y-axis) on the basis of SyMRI-generated (A and B) and conventionally acquired MR imaging data (C and D). Rater 1: A and C; rater 2: B and D.

$-0.349, P = .266$), R1 ($r = 0.363, P = .247$), T2R ($r = -0.461, P = .131$), R2 ($r = 0.567, P = .054$), PD ($r = -0.187, P = .561$), or MR imaging SI ($r = -0.376, P = .229$) determined in the midbrain (Fig 4 and Online Supplemental Data).

DISCUSSION

In this study, a novel quantitative MR imaging technique was used in prenatal neuroimaging. Due to the time-consuming acquisition of MDME sequences, the investigated approach was commonly limited by fetal motion. However, in a certain fraction of successful acquisitions, this technique provides multiple MR imaging data based on a single scan. The results presented here suggest that

provided that an MDME sequence acquisition of sufficient quality is feasible, SyMRI-based image data supply additional multiparametric information to the assessment of fetal brain maturation.

The prenatal radiologic assessment of brain maturity is based on morphologic features and changes in physical tissue properties that lead to MR signal alterations.^{23,26} Cortical development begins in the first trimester of pregnancy by cell proliferation in the ganglionic eminence, followed by neuronal migration through the hemispheres to the surface of the brain.^{9,23,27} With time, postmigrational maturation becomes evident by opercularization, gyration, and sulcation.^{28,29} In fetuses, primarily myelination processes alter the appearance of white matter.^{30,31} Myelin is first seen in the spinal

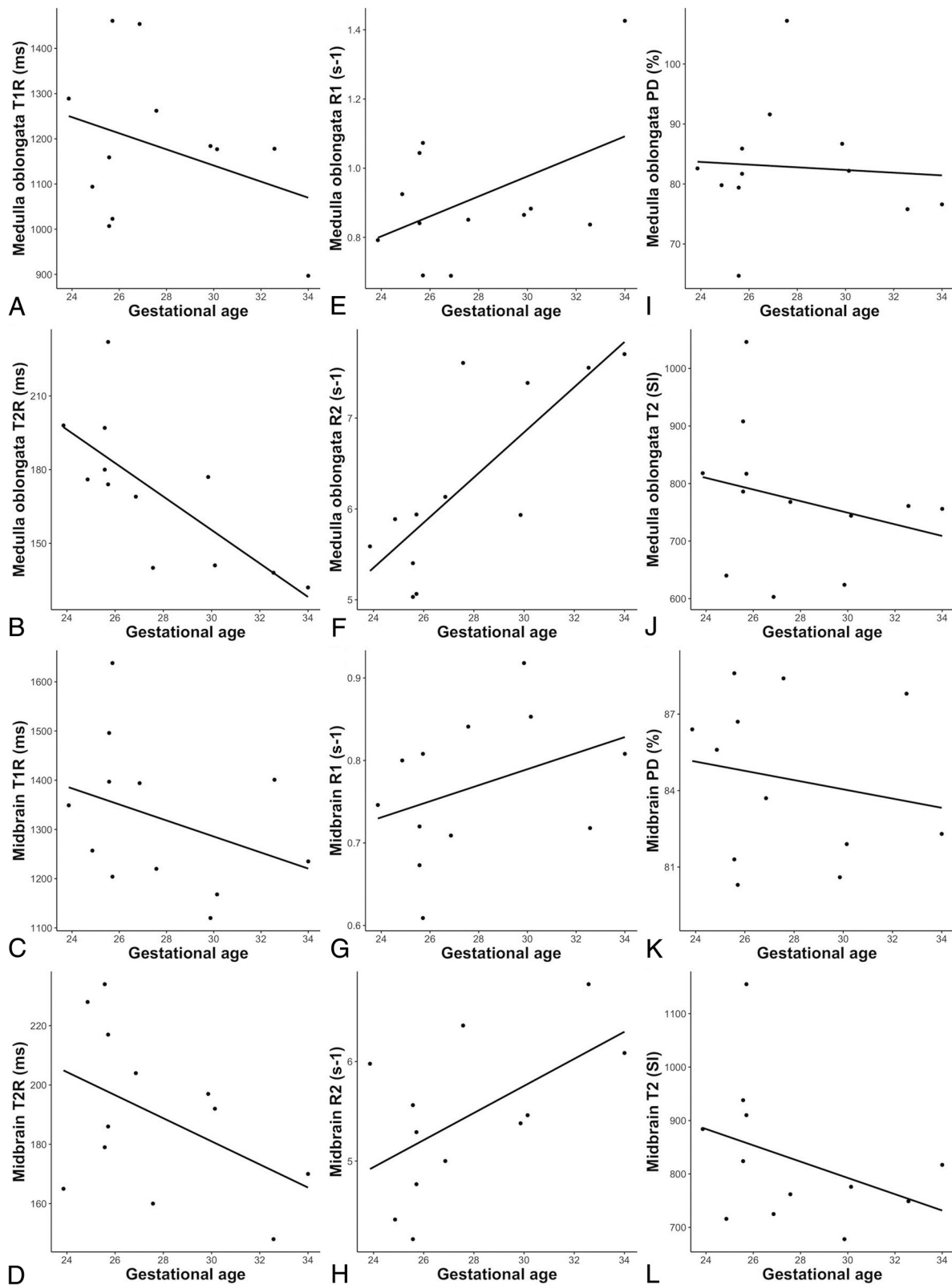


FIG 4. Pearson correlation between GA at MR imaging (x-axis) and quantitative MR imaging metrics (y-axis) determined by rater 1 (medulla oblongata [A, B, E, F, I, J]; midbrain [C, D, G, H, K, L]).

cord and proceeds rapidly cephalad in its dorsal portions.²⁶ In the sixth month of pregnancy, myelination is already detectable in the brain stem.²⁶ At 32 weeks of gestation, myelin-induced MR signal

changes appear supratentorially.^{26,32} Thus, cerebral development progresses through a predictable pattern, underlying the scoring system used in this study.^{15,23}

The assessment of fetal brain maturity based on SyMRI-generated and conventionally acquired MR imaging data revealed comparable results. However, overall, both investigating radiologists reported a higher level of confidence when structural aspects of brain maturation were evaluated on the basis of standard-of-care images, because this technique achieves higher spatial resolution. Most interesting, relatively high levels of confidence were observed when SyMRI-generated maps were available for the evaluation of brain myelination. Quantitative MR imaging mapping has already been proved beneficial for the qualitative assessment of neonatal brain myelination because the color-coding visualizes myelin-induced changes more clearly.¹⁵ The availability of various MR imaging maps for the evaluation of myelination might allow a more consistent neuroradiologic assessment of fetal brain maturity. In the present study, good/excellent concordances were observed between the raters when SyMRI-generated data were used for the evaluation of brain maturation.^{25,33} In contrast, on the basis of the assessment of conventionally acquired MR imaging contrasts, there was only moderate/fair agreement.^{25,33}

However, future development in sequence acceleration and *k*-space sampling are needed to improve the applicability of this technique in a clinical, fetal imaging setting.^{34,35} Nonetheless, the principle of MDME-based postprocessing would be of great benefit in prenatal imaging. Moreover, this technique provides information about tissue-specific properties, which enables the characterization of brain myelination by a quantitative approach.^{11,17}

In fetuses, the maximum quantities of myelin deposition are detectable in the brain stem.^{26,32} Thus, this region best reflects myelin-induced changes in tissue-specific properties. These physical characteristics are linked to visually perceptible MR imaging SI values, which serve as the basis for the qualitative evaluation of brain myelination.²⁶ However, there was only a nonsignificant decrease of the T2 SI values of the brain stem. This finding highlights the limitations of a visual evaluation of myelination based on conventional MR imaging contrasts.¹⁵ Most interesting, significant changes in T2-relaxation parameters of the medulla oblongata were found within the developing brain stem. There is evidence that the tightening of fully developed myelin sheaths induces T2R-shortening/R2-prolongation.³⁶⁻³⁸ The medulla oblongata shows beginning myelination at 24 weeks' GA.²⁶ Hence, in contrast to other substructures of the brain stem, this section already contains a relatively huge amount of fully developed fibers at the end of the third trimester.^{26,32} This fact could also explain that T2R-shortening and R2-prolongation were less pronounced in the midbrain. However, even though T1 MR imaging metrics proved sufficient to quantify brain myelination in neonates, T1R/R1 did not reveal significant changes prenatally.¹¹ Generally, similar to T1R/T2R, the PD decreases as myelin development proceeds.³⁰ In this study, there were no significant correlations between GA and spin density, confirming that PD does not allow a reliable quantitative characterization of brain myelination at early developmental stages.^{11,30}

Delayed brain maturation is associated with neuropsychiatric disorders.^{39,40} Quantitative MR imaging techniques generate valuable image data for the qualitative assessment of fetal brain maturity. Furthermore, these MR imaging data provide novel imaging biomarkers that allow a more differentiated assessment

of prenatal brain development. The evaluation of fetal brain maturity is considered challenging in clinical neuroradiology, and current qualitative assessment strategies are limited by the low sensitivity of conventional MR imaging to small myelin quantities.²⁶ Thus, imaging modalities that enable a more reliable characterization of early developmental stages are greatly needed because these may help clinicians predict future neurodevelopmental disabilities. Quantitative MR imaging metrics could provide the opportunity to track prenatal brain maturation and detect developmental anomalies at an early stage, even though these subtle signal alterations may not be detected qualitatively.²⁶ However, this topic was outside the scope of this study but should be addressed in the future.

This study has several limitations. By default, the fetal MR imaging protocol did not include axial T1-weighted/snapshot inversion recovery MR image acquisitions, limiting a direct comparison of both imaging modalities to a certain extent. The investigated cohort was small and included pathologic brain scans. Furthermore, the limited sample impeded a reliable between-group comparison (fetuses with normal versus pathologic brains). Although only MDME-based image data of superior quality were included in this study, movement-related artifacts were still present in most cases. These limitations might have had an impact on both qualitative and quantitative analyses. Although strong correlations were observed, there is still an impact of movement-related artifacts on qualitative and quantitative analysis that needs to be clearly stated. Nonetheless, the results presented in this work are in line with findings of previous studies that investigated the characteristics of tissue-specific MR imaging properties at the early stages of cerebral development.^{11,30}

CONCLUSIONS

The results of this study indicate that given ideal imaging conditions, MDME-based image data allow a qualitative assessment of maturity-related changes of the fetal brain in utero. In addition, this method makes tissue-specific quantitative information available and, therefore, provides quantitative imaging biomarkers for fetal neuroimaging. Future technical advances in accelerating multiecho sequence acquisitions will help to address current fetal motion-related limitations of this approach. Together with other recent advances in multicontrast, multiparametric estimation techniques such as Strategically Acquired Gradient Echo (STAGE),⁴¹ our data indicate that this line of research is promising and is likely to evolve as a new radiologic strategy to provide complementary MR imaging information to the continuously improving quality of fetal sonography.

Disclosures: Gudrun Mayr-Geisl—UNRELATED: Employment: Medical University of Vienna, Department of Neurosurgery, Comments: University Assistant. Mariana C. Diogo—RELATED: Grant: Austrian Science Fund*; Support for Travel to Meetings for the Study or Other Purposes: Austrian Science Fund*; UNRELATED: Employment: Hospital Garcia de Orta, in the meantime, Comments: working as a neuroradiologist. Gregor Kasprian—UNRELATED: Employment: Medical University of Vienna, Comments: employed as Faculty; Grants/Grants Pending: Austrian Science Fund, Comments: I 3925-B27. *Money paid to the institution.

REFERENCES

1. Bonacquisti L. **Antenatal screening: the first and second trimester.** *Aust Fam Physician* 2011;40:785–87 [Medline](#)

2. Whitworth M, Bricker L, Mullan C. **Ultrasound for fetal assessment in early pregnancy.** *Cochrane Database Syst Rev* 2015;2015:CD007058 [CrossRef Medline](#)
3. Sylvan K, Ryding EL, Rydhstroem H. **Routine ultrasound screening in the third trimester: a population-based study: late ultrasound screening and prognosis.** *Acta Obstet Gynecol Scand* 2005;84:1154–58 [CrossRef Medline](#)
4. Karim JN, Roberts NW, Salomon LJ, et al. **Systematic review of first-trimester ultrasound screening for detection of fetal structural anomalies and factors that affect screening performance.** *Ultrasound Obstet Gynecol* 2017;50:429–41 [CrossRef Medline](#)
5. Malinger G, Paladini D, Haratz KK, et al. **ISUOG practice guidelines (updated): sonographic examination of the fetal central nervous system, Part I: performance of screening examination and indications for targeted neurosonography.** *Ultrasound Obstet Gynecol* 2020;56:476–84 [CrossRef Medline](#)
6. Malinger G, Kidron D, Schreiber L, et al. **Prenatal diagnosis of malformations of cortical development by dedicated neurosonography.** *Ultrasound Obstet Gynecol* 2007;29:178–91 [CrossRef Medline](#)
7. Whitby EH, Paley MN, Sprigg A, et al. **Comparison of ultrasound and magnetic resonance imaging in 100 singleton pregnancies with suspected brain abnormalities.** *BJOG* 2004;111:784–92 [CrossRef Medline](#)
8. Whitby E, Paley MN, Davies N, et al. **Ultrafast magnetic resonance imaging of central nervous system abnormalities in utero in the second and third trimester of pregnancy: comparison with ultrasound.** *BJOG* 2001;108:519–26 [CrossRef Medline](#)
9. Jarvis DA, Griffiths PD. **Current state of MRI of the fetal brain in utero.** *J Magn Reson Imaging* 2019;49:632–46 [CrossRef Medline](#)
10. Rix A, Lederle W, Theek B, et al. **Advanced ultrasound technologies for diagnosis and therapy.** *J Nucl Med* 2018;59:740–46 [CrossRef Medline](#)
11. Schmidbauer V, Dovjak G, Geisl G, et al. **Impact of prematurity on the tissue properties of the neonatal brainstem: a quantitative MR approach.** *AJNR Am J Neuroradiol* 2021;42:581–89 [CrossRef Medline](#)
12. Deoni SCL, Peters TM, Rutt BK. **High-resolution T1 and T2 mapping of the brain in a clinically acceptable time with DESPOT1 and DESPOT2.** *Magn Reson Med* 2005;53:237–41 [CrossRef Medline](#)
13. Deoni SCL, Mercure E, Blasi A, et al. **Mapping infant brain myelination with magnetic resonance imaging.** *J Neurosci* 2011;31:784–91 [CrossRef Medline](#)
14. McKenzie CA, Chen Z, Drost DJ, et al. **Fast acquisition of quantitative T2 maps.** *Magn Reson Med* 1999;41:208–12 [CrossRef Medline](#)
15. Schmidbauer V, Geisl G, Diogo M, et al. **SyMRI detects delayed myelination in preterm neonates.** *Eur Radiol* 2019;29:7063–72 [CrossRef Medline](#)
16. Schmidbauer V, Geisl G, Diogo MC, et al. **Validity of SyMRI for assessment of the neonatal brain.** *Clin Neuroradiol* 2021;31:315–23 [CrossRef Medline](#)
17. Warntjes JB, Leinhard OD, West J, et al. **Rapid magnetic resonance quantification on the brain: optimization for clinical usage.** *Magn Reson Med* 2008;60:320–29 [CrossRef Medline](#)
18. McAllister A, Leach J, West H, et al. **Quantitative synthetic MRI in children: normative intracranial tissue segmentation values during development.** *AJNR Am J Neuroradiol* 2017;38:2364–72 [CrossRef Medline](#)
19. Tanenbaum LN, Tsiouris AJ, Johnson AN, et al. **Synthetic MRI for clinical neuroimaging: results of the Magnetic Resonance Image Compilation (MAGiC) prospective, multicenter, multireader trial.** *AJNR Am J Neuroradiol* 2017;38:1103–10 [CrossRef Medline](#)
20. Prayer D, Malinger G, Brugger PC, et al. **ISUOG practice guidelines: performance of fetal magnetic resonance imaging.** *Ultrasound Obstet Gynecol* 2017;49:671–80 [CrossRef Medline](#)
21. Hagiwara A, Warntjes M, Hori M, et al. **SyMRI of the brain: rapid quantification of relaxation rates and proton density, with synthetic MRI, automatic brain segmentation, and myelin measurement.** *Invest Radiol* 2017;52:647–57 [CrossRef Medline](#)
22. Kang KM, Choi SH, Kim H, et al. **The effect of varying slice thickness and interslice gap on T1 and T2 measured with the multidynamic multiecho sequence.** *MRMS* 2019;18:126–33 [CrossRef Medline](#)
23. Vossough A, Limperopoulos C, Putt ME, et al. **Development and validation of a semiquantitative brain maturation score on fetal MR images: initial results.** *Radiology* 2013;268:200–07 [CrossRef Medline](#)
24. Garel C, Chantrel E, Brisse H, et al. **Fetal cerebral cortex: normal gestational landmarks identified using prenatal MR imaging.** *AJNR Am J Neuroradiol* 2001;22:184–89 [Medline](#)
25. Cicchetti D. **Guidelines, criteria, and rules of thumb for evaluating normed and standardized assessment instruments in psychology.** *Psychol Assess* 1994;6:284–90 [CrossRef](#)
26. van der Knaap MS, Barkhof F, Valk J. *Magnetic Resonance of Myelination and Myelin Disorders.* 3rd ed. Springer-Verlag; 2005
27. Prayer D, Kaspran G, Krampfl E, et al. **MRI of normal fetal brain development.** *Eur J Radiol* 2006;57:199–216 [CrossRef Medline](#)
28. van der Knaap MS, van Wezel-Meijler G, Barth PG, et al. **Normal gyration and sulcation in preterm and term neonates: appearance on MR images.** *Radiology* 1996;200:389–96 [CrossRef Medline](#)
29. Poon LC, Sahota DS, Chaemsaitong P, et al. **Transvaginal three-dimensional ultrasound assessment of Sylvian fissures at 18–30 weeks' gestation.** *Ultrasound Obstet Gynecol* 2019;54:190–98 [CrossRef Medline](#)
30. Lee SM, Choi YH, You SK, et al. **Age-related changes in tissue value properties in children: simultaneous quantification of relaxation times and proton density using synthetic magnetic resonance imaging.** *Invest Radiol* 2018;53:236–45 [CrossRef Medline](#)
31. Ding XQ, Kucinski T, Wittkugel O, et al. **Normal brain maturation characterized with age-related T2 relaxation times: an attempt to develop a quantitative imaging measure for clinical use.** *Invest Radiol* 2004;39:740–46 [CrossRef Medline](#)
32. Yakovlev P, Lecours A. The myelogenetic cycles of regional maturation of the brain. In: Minkowski A, ed. *Regional Development of the Brain in Early Life.* Blackwell; 1967:3–70
33. Koo TK, Li MY. **A guideline of selecting and reporting intraclass correlation coefficients for reliability research.** *J Chiropr Med* 2016;15:155–63 [CrossRef Medline](#)
34. Roy CW, Seed M, Macgowan CK. **Accelerated MRI of the fetal heart using compressed sensing and metric optimized gating.** *Magn Reson Med* 2017;77:2125–35 [CrossRef Medline](#)
35. Senel LK, Kilic T, Gungor A, et al. **Statistically segregated k-space sampling for accelerating multiple-acquisition MRI.** *IEEE Trans Med Imaging* 2019;38:1701–14 [CrossRef Medline](#)
36. Wang S, Ledig C, Hajnal JV, et al. **Quantitative assessment of myelination patterns in preterm neonates using T2-weighted MRI.** *Sci Rep* 2019;9:12938 [CrossRef Medline](#)
37. Barkovich AJ, Lyon G, Evrard P. **Formation, maturation, and disorders of white matter.** *AJNR Am J Neuroradiol* 1992;13:447–61 [Medline](#)
38. Dubois J, Dehaene-Lambertz G, Kulikova S, et al. **The early development of brain white matter: a review of imaging studies in fetuses, newborns and infants.** *Neuroscience* 2014;276:48–71 [CrossRef Medline](#)
39. Wu Y, Stoodley C, Brossard-Racine M, et al. **Altered local cerebellar and brainstem development in preterm infants.** *Neuroimage* 2020;213:116702 [CrossRef Medline](#)
40. Fitzgerald E, Boardman JP, Drake AJ. **Preterm birth and the risk of neurodevelopmental disorders: is there a role for epigenetic dysregulation?** *Curr Genomics* 2018;19:507–21 [CrossRef Medline](#)
41. Qu F, Sun T, Chen Y, et al. **Fetal brain tissue characterization at 1.5 T using STrategically Acquired Gradient Echo (STAGE) imaging.** *Eur Radiol* 2021;31:5586–94 [CrossRef Medline](#)